Chromosoma (2005) 114: 54–66
DOI 10.1007/s00412-005-0339-3

RESEARCH ARTICLE

A. A. Gortchakov · H. Eggert · M. Gan · J. Mattow · I. F. Zhimulev · H. Saumweber

Chriz, a chromodomain protein specific for the interbands of *Drosophila melanogaster* polytene chromosomes

Received: 8 December 2004 / Revised: 15 March 2005 / Accepted: 16 March 2005 / Published online: 9 April 2005

Abstract Polytene interphase chromosomes are compacted into a series of bands and interbands reflecting their organization into independent chromosomal domains. In order to understand chromosomal organization, we set out to study the role of proteins that are selective for interbands. Here we describe the *Drosophila melanogaster* chromodomain protein Chriz that is coimmunoprecipitated with the zinc finger protein Z4. Both proteins colocalize exclusively to the interbands on *Drosophila* polytene chromosomes. Like Z4, Chriz is ubiquitously expressed throughout development and is associated with chromatin in all interphase nuclei. Following dissociation from chromatin, early in mitosis Chriz binds to the centrosomes and to the mitotic spindle. Newly induced amorphic *Chriz* alleles are early lethal, and ubiquitous overexpression of Chriz is lethal as well. Available *Chriz* hypomorphs which survive until pupal stage have a normal chromosomal phenotype. Reducing Z4 protein does not affect Chriz binding to polytene chromosomes and vice versa. Z4 is still chromosomally bound when Chriz protein is depleted by RNA interference.

Communicated by H. Jäckle

A. A. Gortchakov · I. F. Zhimulev
Institute of Cytology and Genetics,
Siberian Branch of Russian Academy of Sciences,
Novosibirsk, Russia

H. Eggert · M. Gan · H. Saumweber (✉)
Cytogenetics Division,
Institute of Biology,
Humboldt University,
Berlin, Germany
e-mail: hsaumweber@gmx.net
Tel.: +49-30-20938178
Fax: +49-30-20938177

J. Mattow
Max Planck Institute for Infection Biology,
Berlin, Germany

Introduction

Eukaryotic chromatin is organized into independent functional units called chromosomal domains. Topological closed domains were demonstrated by biochemical methods (Benyajati and Worcel 1976; Igo-Kemenes and Zachau 1978) and were suggested by the cytology of mitotic and meiotic chromosomes (Paulson and Laemmli 1977; Callan 1987). Similarly, the banded structure of polytene interphase chromosomes is interpreted as evidence for looped domains.

In *Drosophila* larvae, like in many other insects, polytene chromosomes result from endoreplication cycles when the replicated chromatids do not separate by mitosis but remain closely associated by homolog pairing. As a consequence, interphase chromosome organization becomes apparent where phase dark bands are separated by phase light interbands, resulting in a species-specific banding pattern. A similar pattern of bands is consistently observed in all polytene tissues down to the lowest level of polyteny amenable to cytological analysis. Thus, the band/interband pattern reflects a common structural organization of interphase chromosomes in general. Each band/interband unit in *Drosophila melanogaster* contains, on average, 60 kb DNA and is considered to reflect a chromosomal domain. The bands constitute the bulk of the domain including one or several transcription units. Bands may show a dynamic behavior due to the transcriptional activity of their resident genes. For instance, the *D. melanogaster* heat shock locus in band 87A7 decondenses into a large puff following an increase in temperature to 37°C and similar change in structure can be observed for many ecdysone regulated genes. In contrast, our knowledge on interbands is limited and several different views were proposed for interband function.

Using various sources and methods, various groups estimated the amount of interband DNA between 1% and 25% of total DNA (reviewed in Zhimulev 1996). Although the interbands contain less DNA, bands and interbands comprise roughly the same length, indicating differences in packing ratios. By cytophotometry and high-resolution in situ hybridization data, the DNA packaging ratio in bands

was determined as 60- to 100-fold and that of interbands to about 5- to 8-fold (Beermann 1972; Rykowski et al. 1988). Thus, interband chromatin structure is likely a 10-nm nucleosome fiber, whereas chromatin in bands is condensed at least into 30-nm fibers (Rykowski et al. 1988).

Due to their decompacted state, interbands have long been hypothesized as the sites of transcriptional activity and nascent RNA molecules as well as RNA polymerase II were localized to interbands (Zhimulev and Belyaeva 1975; Semeshin et al. 1979; Plagens et al. 1976; Sass 1982; Sass and Bautz 1982). However, the total length of interbands has insufficient coding capacity and in many cases transcription units were localized to bands. Moreover, selective staining of the active elongating form of RNA polymerase II is restricted to puffs and minipuffs (Weeks et al. 1993; Gerber et al. 2001), unlike the more general puff and interband staining observed earlier (Plagens et al. 1976). Alternatively, interbands were considered to contain the regulatory regions and transcription initiation sites of genes located in adjacent bands. Supporting this view, Rykowski et al. (1988) demonstrated that the *Notch* transcribed region is located within the band 3C7 and the *Notch* promoter and the upstream regulatory regions are contained within the 3C6-C7 interband.

Intuitively, the difference in compaction between bands and interbands suggests the existence of boundaries between the two elements. The chromosomal binding of boundary element proteins in interbands and the mapping of regulatory elements suggest that interbands indeed provide boundaries of chromosomal domains. The heat shock locus at 87A7 contains two divergently transcribed *hsp70* genes that are flanked by specialized chromatin structure elements *scs* and *scs′*, respectively (Udvardy et al. 1985). Both elements confer position-independent expression on *Drosophila* transgenes and are functional as enhancer blockers in transgene expression (Kellum and Schedl 1991, 1992). Boundary elements with similar properties have been localized to the interband 3C6-3C7 preceding the *Notch* locus (Vazquez and Schedl 2000). The *scs′* activity is mediated by the Boundary Element Associated Factor 32 (BEAF-32A, B; Zhao et al. 1995; Hart et al. 1997). The BEAF-32 proteins are localized at numerous interbands on polytene chromosomes and their suggested boundary function at these sites has been proven in some cases (Cuvier et al. 1998).

To learn more about the formation of interbands and chromosomal boundaries, a study of interband proteins and their mutual interactions with the corresponding genomic DNA sequences is urgently required. At present, data accurately matching the DNA sequences from the *Drosophila* genome project with the cytology of polytene chromosomes are rather limited. The 3C6-7 is the only example of an interband mapped at a molecular level (Rykowski et al. 1988 and references therein). Detailed knowledge on interband proteins is a prerequisite to understand interband structure and function, and antibodies to such proteins would provide useful handles to isolate interband sequences by ChIP analysis. Besides the BEAF32 isoforms A, B, only a few interband-specific proteins are known so far. The tandem kinase Jil-1, besides its function in dosage compensation, plays a role in the maintenance of interbands, since removing *Jil-1* function resulted in highly compacted polytene chromosomes lacking any banded appearance (Jin et al. 1999, 2000). The Brahma complex localizes to puffs and many interbands (Armstrong et al. 2002; Mohrmann et al. 2004), but its role in interband formation is not known.

We recently described the Z4 protein as an interband-specific zinc finger protein, which is involved in the establishment or maintenance of the alternating band/interband pattern. Reduction of the amount of Z4 results in a progressive disintegration of the banded structure of polytene chromosomes. However, in contrast to *Jil-1*, *Z4* mutant chromosomes were not compacted but had lost their banded organization and had a cloudy decompacted appearance (Eggert et al. 2004).

To identify potential interacting partners of Z4, coimmunoprecipitation with a Z4-specific antibody was carried out, and a chromodomain protein with an apparent molecular weight of about 140 kDa was identified—which we named Chriz, for *Chr*omodomain protein *i*nteracting with *Z*4 (Eggert et al. 2004). The chromodomain is a conserved motif found in many nuclear proteins involved in chromatin organization from yeast to humans. This paper describes the results of our molecular and cytogenetic analysis of the interband-specific protein Chriz.

Materials and methods

Drosophila stocks and genetics

Fly stocks were kept on standard *Drosophila* cornmeal–molasses medium at 25°C unless otherwise indicated. *Oregon-R* was used as a wild-type stock. The *KG6256* and *KG3258* stocks were obtained from the laboratory of Dr. H. Bellen (Bellen et al. 2004), *sh044* and *Df(3L)79E-F* were kindly provided by Dr. S. Oh (Oh et al. 2003) and Dr. Ruohola-Baker (Clegg et al. 1997), respectively, whereas all other stocks were obtained from Bloomington Stock Center. T80-GAL4 (Wilder and Perrimon 1995), Act-GAL4 (Ito et al. 1997) and Da-GAL4 (Wodarz et al. 1995) transgene lines were used to drive the ubiquitous expression of UAS transgenes. G14.1–GAL4 is a salivary gland-specific GAL4 driver, which is active in gland secretion epithelia from stage 12 of embryo development into pupal stages (Dr. U. Hinz, Köln). Sgs3-GAL4 (Cherbas et al. 2002) drives expression in salivary glands of mid-third instar larvae. Genetic markers and balancers not described in this work can be found in FlyBase (The FlyBase Consortium 2003) and in Lindsley and Zimm (1992). *Drosophila* species (*D. mauritiana*, *D. erecta*, and *D. takahashii*) used for the comparative molecular evolutionary analysis were kept in the laboratory at Novosibirsk for a long time.

The excision of *P{SUPor-P}* (Roseman et al. 1995) and *P{lacW}* (Bier et al. 1989) transposons was induced by crossing to a transposase stock w^{1118}; *CyO*/*Sp*; *PΔ2-3*, *Sb* ry^{506}/*TM6*, *Ubx*. White-eyed F_2 males were collected and crossed individually to the *y w*; *CyO*/*If*; *MKRS*, *Sb*/*TM6B*, *Tb*, *Hu* females; then their progeny were established

as balanced stocks and further tested for the reversion and lethality. A stock bearing the insertion of the pWR-gChriz transposon (see below) on the second chromosome was used for the rescue experiments.

Molecular procedures

All molecular procedures were performed essentially as previously described (Sambrook and Russell 2001). All DNA-modifying enzymes were purchased from New England Biolabs. Sequencing was done on the ABI PRISM 310 Genetic Analyzer (Applied Biosystems).

RNA from different developmental stages was isolated using Trizol (Gibco BRL). Poly(A)$^+$ RNA was purified using MicroPoly(A)Purist mRNA Purification Kit (Ambion), and subjected to Northern blot analysis with DNA probes prepared from the GH27095 cDNA clone and the rp49 sequence present in pHR0.6 (O'Connell and Rosbash 1984). Primer sequences used for the amplification of *Chriz* genomic sequences in different *Drosophila* species are available upon request.

Constructs for transformations

A 7.1-kb genomic *Sca*I–*Eco*RI fragment encompassing the entire *Chriz* gene and a partial sequence of the neighboring *Ssl*I gene (Fig. 1b) was cloned from the RP98-48E5 BAC clone (Hoskins et al. 2000) into pBluescript cut with *Eco*RV and *EcoR*I. The cloned insert was excised with *Kpn*I and *Spe*I, and subcloned into similarly cut *Drosophila* transformation vector pWhiteRabbit (a kind gift from N. Brown) to yield a P$\left[WR.w^{+mC}, Chriz^{+t7.1}\right]$ transposon (designated as pWR-gChriz).

The Chriz protein coding sequence corresponding to amino acids 27–926 was PCR amplified from the cDNA clone GH27095 (available from Invitrogen) with primers ChrFNot 5′-TAGGGCGGCCGCGACGTTCTTGTATGTG GACG-3′ and ChrR0 5′-GCTCTAGATTACGTTGGGATG TTGAGCGTC-3′ and placed in pBluescriptII/*Eco*RV to obtain pBlue-Chriz. Then it was reexcised as a *Not*I–*Sal*I fragment from pBlue-Chriz and cloned into *Drosophila* transformation vector pUAST-myc-his (J. Kaltenhäuser, H. Eggert, unpublished data) cut with *Not*I and *Xho*I. Thus, *Chriz* CDS was inserted downstream to and in-frame with the sequences coding for two epitope tags, 6xHis, and 3xMyc, under control of the UAS elements of pUAST (Brand and Perrimon 1993). Upon transformation in the y^1w^1 host strain, several homozygous viable transgenic lines with autosomal insertions of the P[$w^{+mW.hs}$, $UAS_{GAL}hsp70$:*3xmyc-6xhis-Chriz*$^{+2.7}$] transposon (designated as pUAST-myc-his-Chriz) were established.

To obtain Chriz-dsRNAi construct, we first cloned a 927-bp *Bam*HI fragment from pBlue-Chriz into the *Bgl*II site of pEFGP-1. Then we introduced a 1.3-kb *Sac*I–*Sac*II fragment (antisense orientation) from pBlue-Chriz into the construct made to obtain pEGFP-Chriz-dsRNAi. The 2.2-kb *Eco*RI fragment from pEGFP-Chriz-dsRNAi was subsequently placed into the *Eco*RI site of pUAST. The resulting transposon P[UAS-Chriz-dsRNAi] was used to transform flies, and a stock with an insert on the third chromosome was established.

Antibodies and immunocytochemistry

Polyclonal Chriz-specific antibodies were raised in rabbits using the C-terminal half of Chriz (345–926 aa), cloned as a *Bam*HI–*Sal*I fragment from pBlue-Chriz into similarly cut pQE30a (Qiagen) to generate 6xHis-Chriz (345–926) fusion. The fusion protein was expressed in BL21(DE3) *E.*

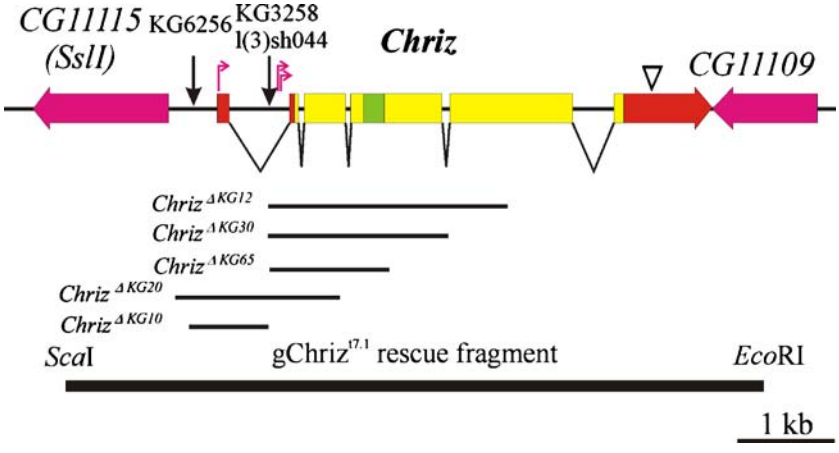

Fig. 1 Molecular map of the *Chriz* locus, P-element insertions and deletions: *Chriz* UTRs are shown in *red* and protein coding regions are represented in *yellow*, the chromodomain is labeled *green*. *Pink arrows* indicate alternative transcription start sites. The *open triangle* indicates the alternative polyadenylation signal. Positions of the adjacent genes *Ssl1* and *CG11109* transcribed from the opposite strand are shown in *purple*. *Vertical black arrows* indicate the P-transposon insertion sites in the stocks *KG6256*, *KG3258* and *sh044*. Sequences deleted by imprecise excision of *P{SUPor-P}* from *KG3258* are shown as *thin black lines*. The genomic clone gChriz$^{+t7.1}$ that complements *ΔKG12* and *ΔKG65* alleles is shown as a *thick black line underneath*

coli cells, affinity purified on Ni-NTA agarose (Qiagen), and injected into two rabbits. Antisera obtained were assayed by Western blotting.

For immunostaining, bleach-dechorionated embryos were fixed in formaldehyde, and further processed as previously described (Eggert et al. 2004). Rabbit anti-Chriz antibodies were used at a 1:1,000 dilution. Secondary anti-rabbit IgG-FITC and -TRITC conjugates were purchased from Dianova (Jackson Imm. Res.), and used at a 1:200 dilution. DNA was counterstained with Hoechst 33258. Immunostaining of formaldehyde fixed Kc cells, whole mount embryos and polytene chromosomes was essentially

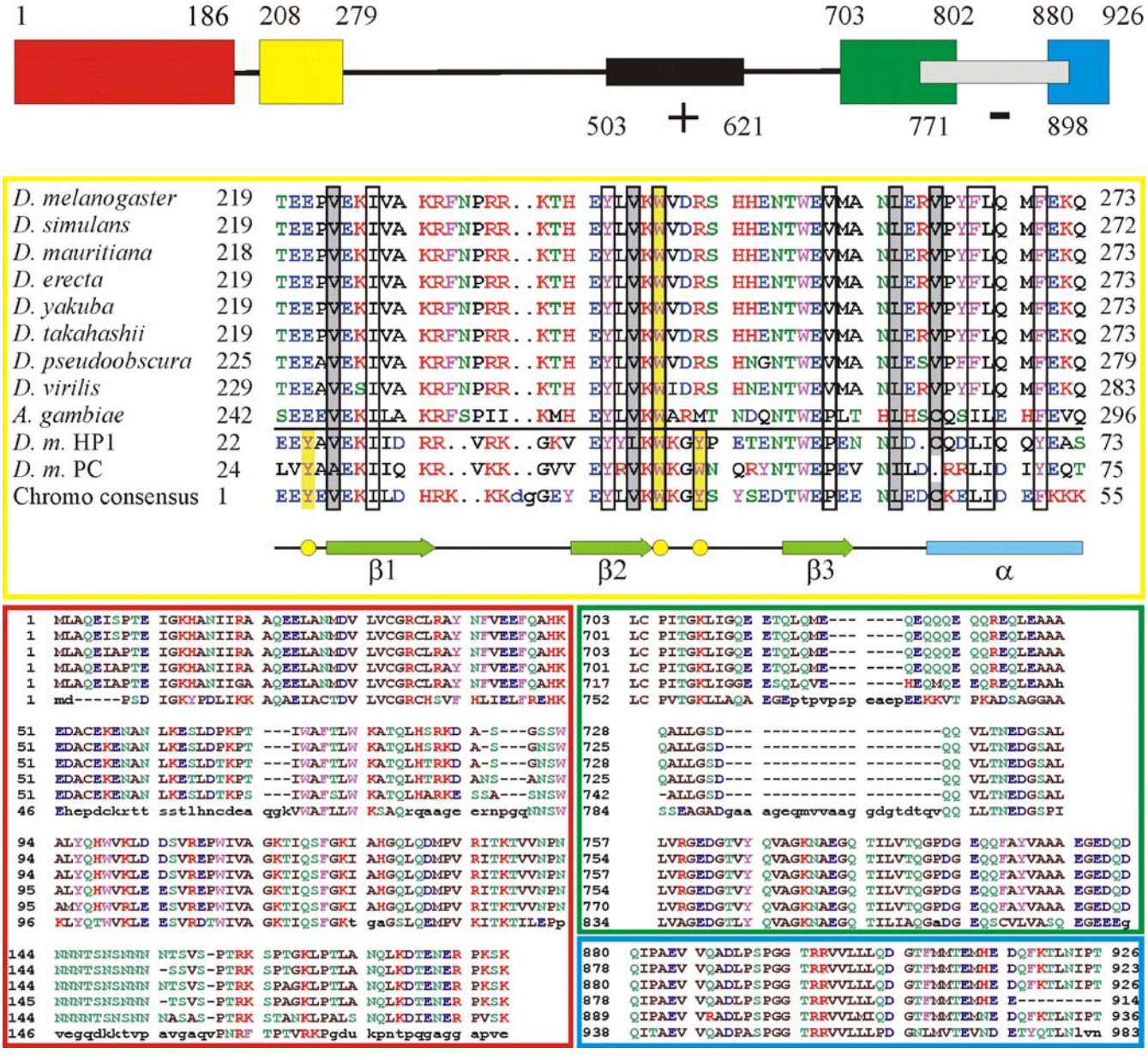

Fig. 2 Chriz domain organization. *Top line*: conserved Chriz regions are shown as *colored rectangles* with sequence information given in the *boxes labeled with the same colors below*. The extent of the domains is given by aa numbers; regions with maximal spacing between positively and negatively charged residues are depicted as *black* and *gray rectangles*, respectively; *yellow box* indicates the chromodomain; alignment of Chriz chromodomain in the dipteran species indicated, and of HP1 and PC chromodomains in *D. melanogaster* was performed using MultiAlin software (Corpet 1988); basic aa are shown in *red*, acidic aa are in *blue*, uncharged aa are in *dark green* and aromatic aa are in *purple*. Location of the conserved β-sheet (*green arrows*) and α-helical regions (*light blue box*) constituting the chromodomain fold as determined for HP1 and PC in *Drosophila* and mouse is given *below the alignment*. Conserved aromatic residues (Y_3, W_{26} and Y_{29} of the consensus) which form the recognition site for the methylated lysine side chain are highlighted in *yellow*, chromodomain residues that make contacts with the n-2 position relatively to the methyllysine (*n*) are shaded in *gray*. Conserved hydrophobic residues that define the fold and set the borders of β-sheets and the α-helix are *boxed*. *Red*, *green* and *blue box*: Chriz regions conserved in *D. melanogaster*, *D. mauritiana*, *D. erecta*, *D. takahashii*, *D. pseudoobscura* and *Anopheles gambiae*. *Alignment* and *coloration* of aa as for the chromodomain

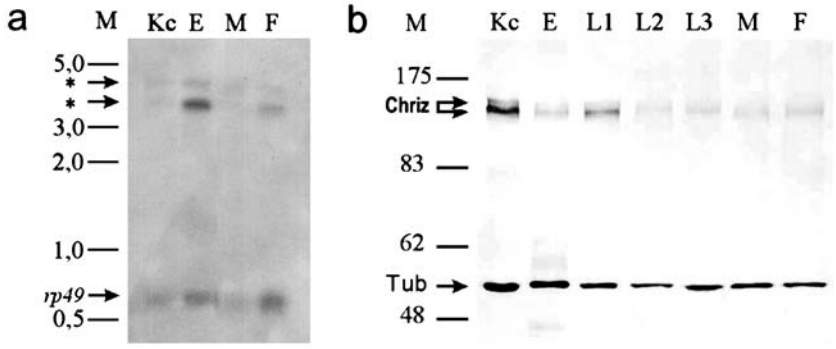

Fig. 3 Chriz expression. **a** Northern blot using polyA+ RNA isolated from *Drosophila* Kc cells (*Kc*), 0–16 h embryos (*E*), male (*M*) and female adults (*F*) was probed with the *Chriz* GH27095 cDNA clone and a rp49 probe as a loading control; the 3.8- and 3.2-kb transcripts are labeled by *asterisk*; note the prevalence of the 3.2-kb transcripts in females and embryos. (M) Molecular weight markers given in kb to the *left*. **b** Western analysis using anti-Chriz antisera at 1,000-fold dilution on protein blots containing Kc cell nuclear proteins (*Kc*), proteins from 0 to 16 h embryos (*E*), first (*L1*), second (*L2*) and third instar larvae (*L3*), and male (*M*) and female adults (*F*), respectively; antitubulin antiserum was used as a loading control. Chriz polypeptides are indicated by *arrows*. The faint Chriz band at 150 kDa MW^{app} is seen most clearly with Kc cell nuclear proteins though it is always present. (M) Molecular weight markers given in kDa MW^{app} to the *left*

carried out as described (Eggert et al. 2004). To visualize the distribution of dhnRNP K (Hrb57A), the monoclonal antibody Q18 was used (Hovemann et al. 2000). Images were taken using appropriate filter combinations with a Zeiss Axiophot equipped with a high-performance CCD camera. For high-resolution analysis, specimens were viewed with a Deltavision Spectris optical sectioning microscope (DeltaVision, Issaquah, USA).

Results

Identification and sequence analysis of Chriz

In our previous analysis of the interband-specific Zn-finger protein Z4 (Eggert et al. 2004), we found that Z4 coimmunoprecipitates several polypeptides, most prominently a protein of an apparent mass of 140 kDa. This protein band

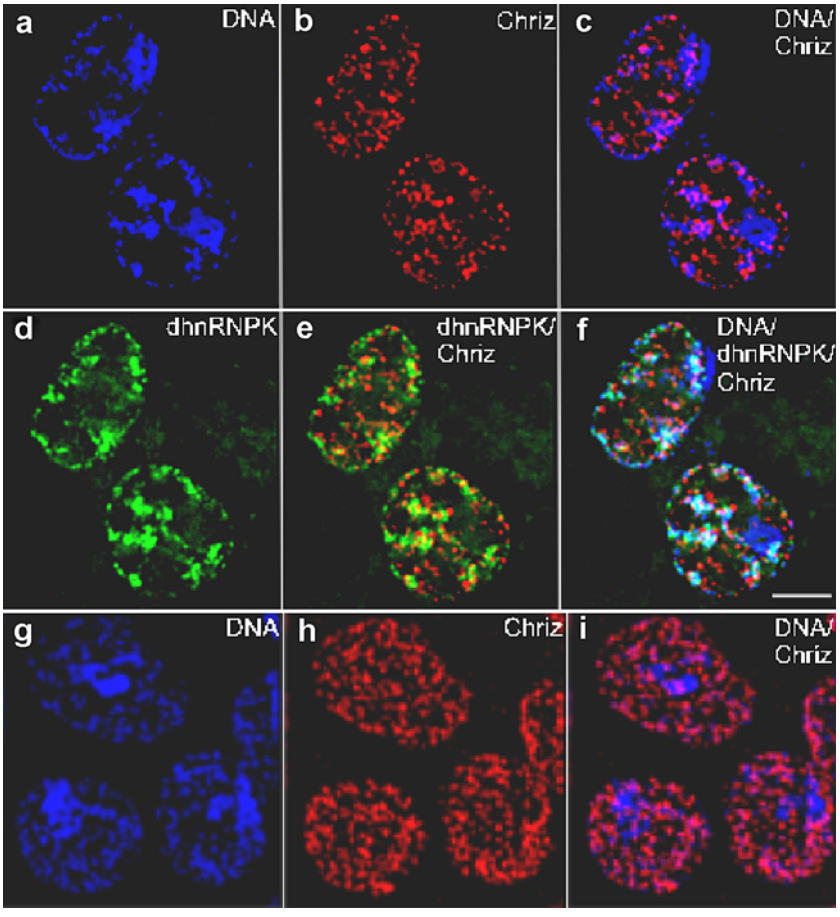

Fig. 4 Chriz distribution in nonpolytene cell nuclei. **a**–**f** Kc cells triple stained by Chriz antisera (*red*), dhn-RNP K (monoclonal ab Q18; *green*) and Hoechst DNA specific dye (*blue*) as indicated; optical section of nuclei stained for **a** DNA, **b** Chriz, **c** DNA and Chriz, **d** dhn-RNP K, **e** Chriz and dhn RNP K, **f** DNA; Chriz and dhn-RNP K; note that Chriz is excluded from large heterochromatic blocks and that Chriz and dhn RNP largely do not overlap. **g**–**i** Imaginal ring cells from the anlage for the adult salivary gland stained as mentioned for **g** DNA, **h** Chriz and **i** DNA and Chriz. *Bar* in **f** is 2.5 μm

was analyzed by MALDI-TOF mass spectrometry and peptide mass maps were searched in a nonredundant database in FASTA format as described previously (Reim et al. 1999). Nineteen (41%) of 46 peptides could be matched with an ORF of a putative gene *CG10712* from the *Drosophila* genome database which corresponds to a total sequence coverage of 27%. In order to prove that we isolated the cognate Z4 interaction partner, CG10712 cDNA was cloned in frame to a myc-his-tag in the pUAST transformation vector (see Materials and methods). On expression in salivary glands using a Sgs3-Gal4 driver line, the tagged fusion protein was localized exclusively in the interbands of polytene chromosomes (Eggert et al. 2004). This pattern perfectly matches that of the Z4 antigen (Eggert et al. 2004), demonstrating that the *CG10712* encodes the desired protein that interacts and colocalizes with Z4 in vivo. We therefore named this gene *Chriz* (Eggert et al. 2004).

Chriz is a single copy gene located in 79F on chromosome 3L close to the centromeric heterochromatin. The gene has three transcriptional start sites, alternative usage of the first intron, and two different polyadenylation sites that are ~0.6 kb apart (Fig. 1; compare FlyBase). The 5′-most start site should result in the expression of a ~3.8-kb transcript. In addition, there are two internal start sites 92 bp apart from each other that would result in two ~3.8-kb transcripts. The alternative polyadenylation site would result in two classes of transcripts differing by 0.6 kb. However, all mRNAs encode the same protein of 926 amino acids with the calculated molecular weight of 101 kDa. Apart from an overrepresentation of glutamine (1.78×) and an underrepresentation of cysteine (0.2×), phenylalanine (0.4×) and tyrosine (0.3×) residues, the amino acid composition of Chriz is that of an average *Drosophila* protein (Smoller et al. 1990).

Blast searches in protein databases (Altschul et al. 1997) revealed a chromodomain, an evolutionary conserved protein module of about 50 amino acids, in the N-terminal part of Chriz (Fig. 2; Paro and Hogness 1991). Chromodomain-containing proteins are widespread among eukaryotes. *D. melanogaster* contains 17 proteins with chromodomains (Rubin et al. 2000). It was demonstrated that chromodomains of Heterochromatin protein 1 (HP1) and Polycomb (PC) mediate the specific recognition of methylated lysine residues K9 and K27 of histone H3, respectively (Nielsen et al. 2002; Fischle et al. 2003). Comparison of the Chriz chromodomain sequence with those of HP1 and PC reveals significant conservation in residues that define the spatial organization characteristic of the chromodomain module (Fig. 2). Nevertheless, two out of the three aromatic residues in chromodomain of HP1/PC that were identified to be

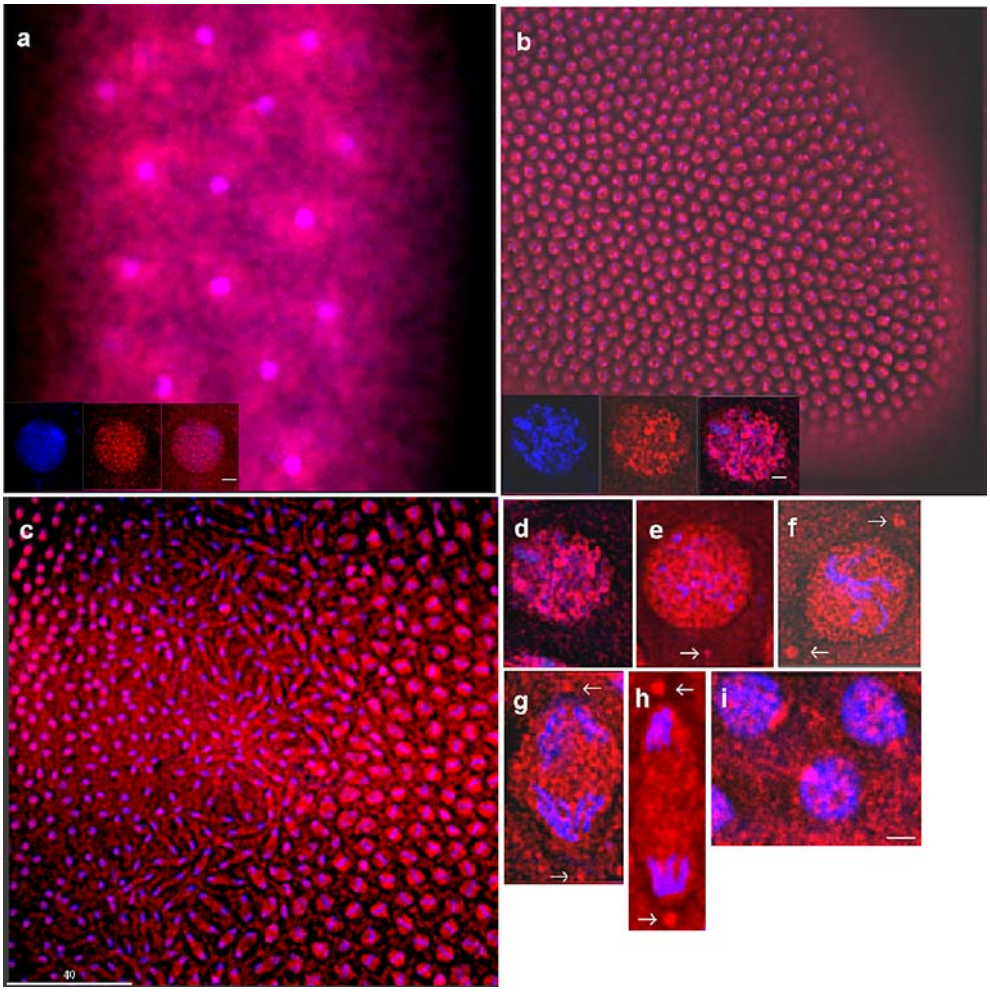

Fig. 5 Chriz binding in interphase and during mitosis of early *Drosophila* embryos. **a** Chriz is present in energids and nuclei of cleavage stage embryos; low-power magnification of embryo at nuclear cycle 6 double stained by Chriz antisera (*red*) and DNA-specific dye Hoechst (*blue*); *inset*: single nucleus of the same embryo at higher magnification stained (from *left* to *right*) for DNA, Chriz or both. **b** Chriz is exclusively nuclear in blastoderm stage embryos at interphase; nuclear cycle 14 embryo was stained as in **a**; *inset*: nuclei at higher magnification. Note the increased granular Chriz staining compared to cleavage nuclei. **c**–**i** Chriz associates with the spindle and the centrosomes during mitosis. **c** Mitotic gradient in a nuclear cycle 13 embryo from late prophase (*right*) to early telophase (*left*); nuclei from representative mitotic stages at higher magnification in **d** interphase, **e** prophase, **f** prometaphase, **g** early and **h** late anaphase, **i** telophase; note the centrosome staining indicated by an *arrow*. *Bar* in **c** 40 μm (for **a**–**c**); *bar* in *inset* of **a**, **b** 1.5 μm; *bar* in **i** 2.5 μm (for **d**–**i**)

crucial for the recognition of histone H3 di- and trimethyllysine are substituted in the chromodomain of Chriz for charged amino acids.

In protein database searches for other potentially conserved Chriz domains, we failed to identify significant homology outside the chromodomain region. Although the protein is exclusively nuclear (see below), no consensus NLS was detected. Since domains important for function often retain their structure in more closely related species, we compared the Chriz coding sequence in different dipteran species. Following PCR amplification we sequenced the *Chriz* gene from *D. mauritiana*, *D. erecta*, and *D. takahashii* (GenBank accession numbers AY273293–AY273295) and compared it with its sequences recently available for *D. simulans*, *D. yakuba*, *D. virilis*, *D. pseudoobscura* and *Anopheles gambiae*. Comparison of the deduced Chriz amino acid sequences allowed us to identify three conserved regions in addition to the chromodomain (aa 208–279): (1) an aminoterminal region (aa 1–186), (2) a strongly conserved domain (aa 703–802) and (3) a carboxyterminal region (880–926). In addition, there were regions whose positive charge (503–621) or negative charge (771–898) was conserved in general between the species (Fig. 2).

Chriz is ubiquitously expressed

Expression of *Chriz* is shown in Fig. 3a on a developmental Northern blot. The *Chriz* RNA is expressed at all stages of development, with a more pronounced expression in embryos and in adult females (see also Arbeitman et al. 2002). The *Chriz* messages of ~3.8 and ~3.2 kb correspond to the two alternately polyadenylated products. The 3.2-kb transcript is more prominent in females and embryos and may be maternally transmitted.

Following expression of Chriz in bacteria, specific rabbit antisera were raised. On Western blots using Kc cell nuclear proteins, both antisera detect a minor band of 150 kDa and a major band of 140 kDa (Fig. 3b). Both are larger than expected from the predicted molecular weight of the Chriz

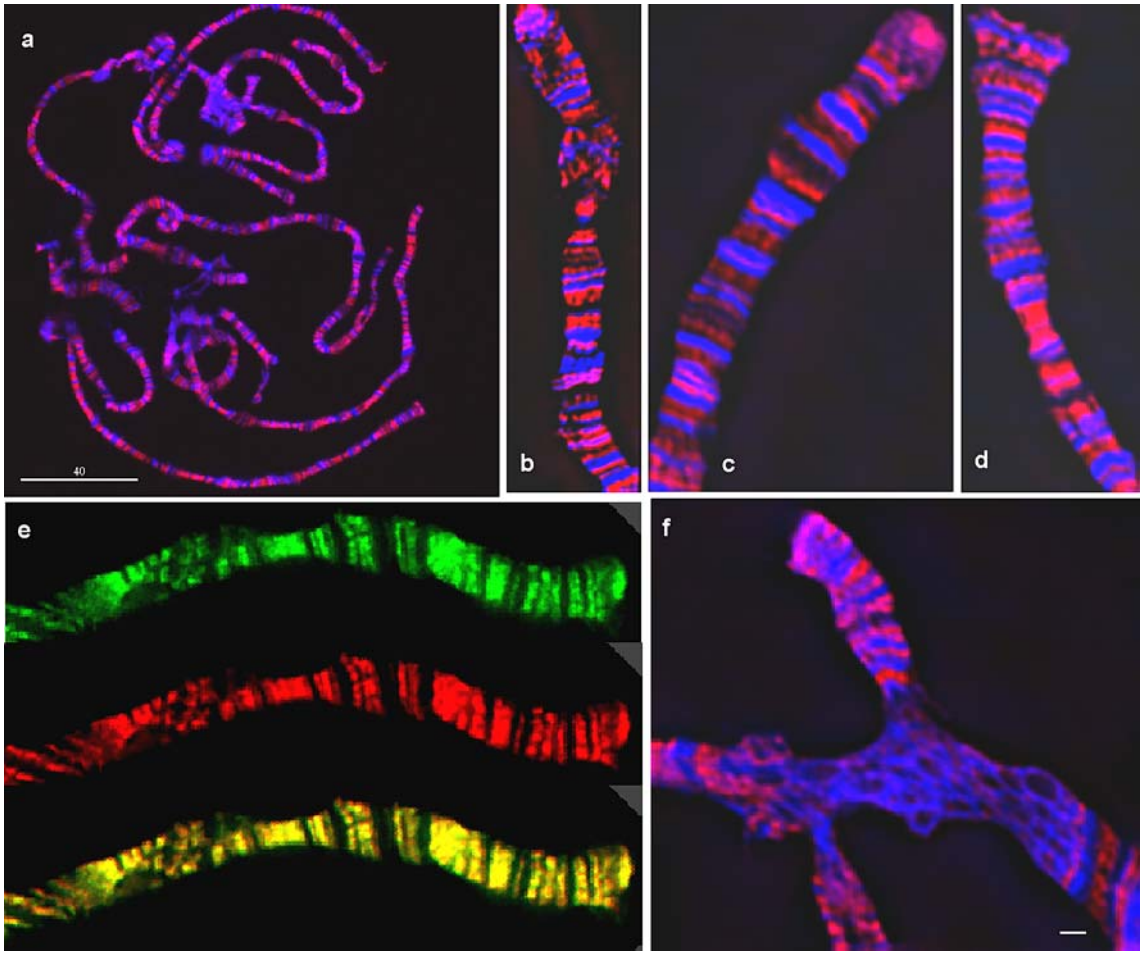

Fig. 6 Chriz is present in interbands of polytene chromosomes and colocalizes with the zinc finger protein Z4. **a** Low-magnification view of a set of polytene chromosomes stained for Chriz (*red*) and DNA (*blue*); **b**–**d**, **f** higher magnification views of **b** distal X chromosome, **c** distal chromosome 2L, **d** distal chromosome 3R and **f** the chromocenter including the fourth chromosome. Chriz (*red*) is located in interbands, DNA stained by Hoechst dye (*blue*) is mainly seen in condensed bands; note the absence of staining at centromeric heterochromatin and the prominent staining at the telomeres of the X, 2L and the fourth chromosome. **e** Z4 and Chriz colocalize on polytene chromosomes; *top*: Z4 (*green*); *middle*: Chriz (*red*); *bottom*: colocalization is demonstrated by the *yellow color* resulting from the overlay of both wavelengths. *Bar* shown in **a** is 40 μm and in **d** 2.5 μm (for **b**–**f**)

protein. Since all possible splice forms suggest only a single ORF, the two forms may represent posttranslational modifications. The same two proteins are present in Kc cells and in embryo, larval and adult stages (Fig. 3b). In contrast to *Chriz* RNA, the protein is not upregulated in embryos and adult females.

On immunostaining Chriz is detected as a nuclear protein in all tissues and organs tested so far. In the *Drosophila* cell line Kc, nuclei are stained in a speckled pattern distinct from that of the condensed DNA (Fig. 4a–c). This pattern is also unlike the speckled distribution previously described for the hnRNPs (Fig. 4d–f). In cleavage stage embryos, in addition to the nuclear labelling, considerable staining is found in the cytoplasmic islands surrounding the nuclei (Fig. 5a). At syncytial blastoderm and later stages the bulk of the protein is present in speckles inside the nuclei, which do not coincide with condensed chromatin. This is most obvious in the apical heterochromatic chromocenter, which is not stained by Chriz antibodies (Fig. 5b). There is no indication for lineage- or tissue-specific staining at these and later stages (data not shown). Similarly, there is staining of all nuclei in imaginal rings, imaginal discs, in brain and ovaries with no indication for tissue specificity (Fig. 4g–h and data not shown).

In early embryos the nuclear localization of Chriz during mitosis is easily observed. During syncytial blastoderm stages its distribution can be observed on mitotic gradients formed in the embryo (Fig. 5c). During prophase Chriz starts dissociating from chromosomes and in metaphase it is mainly present within the nuclear cage with the condensed mitotic chromosomes largely devoid of Chriz (Fig. 5e, f). Other nuclear proteins are detected on metaphase chromosomes using the same fixation conditions (Frasch et al. 1986). Interestingly, starting at prophase Chriz protein is detected at the centrosomes that organize the mitotic spindle outside the nuclei. In early anaphase, when the nuclear envelope is disintegrated (Paddy et al. 1996), Chriz associates with the mitotic spindle (Fig. 5g). Later in anaphase it is still prominent in the spindle region and it begins to accumulate in nuclei at telophase. A similar mitotic distribution was reported by Rath et al. (2004), who identified the same protein by its interaction with the spindle protein Skeletor (see Discussion). The Z4 protein described previously (Eggert et al. 2004) exhibits a very similar distribution during mitosis (data not shown).

Chriz colocalizes with Z4 in interbands

Chriz is detected in many interbands on polytene chromosomes when stained with specific antisera (Fig. 6a–d). However, we note that some interbands do not contain this protein. Certain telomeres, like those of chromosome 2L and the X chromosome, appear more strongly stained (Fig. 6b, c). However, Chriz is absent from bands and it is also largely absent from decondensed puffs. The latter observation is inconsistent with simple models that Chriz binding is a consequence of chromosome decondensation. Chriz is not found at pericentric heterochromatin and the chromocenter core (Fig. 6f), where histone H3 mono-, di- and trimethylated at lysine 9 and 27, respectively were observed (Ebert et al. 2004). Following coimmunostaining with Z4 antibodies and anti-Chriz antisera, it is demonstrated that both proteins essentially colocalize on polytene chromosomes (Fig. 6e). The heat shock region in 87AC was investigated for the presence of Chriz protein before and after 30 min heat shock induction at 37°C (Fig. 7). The puffs at 87A7 and 87C were not stained by the Chriz antibody. Yet, although the interbands in the vicinity of the puff are distorted by breaking up the polytene chromosomes into chromatin bundles, the staining of the Chriz protein is still localized at the flanks of both puffs (Fig. 7b). Interestingly, the heat shock puff 87A7 at its distal border shows significant Chriz binding and less binding at its proximal border, similar to the binding reported for the boundary element-associated factor BEAF 32 (Zhao et al. 1995). The heat shock puff forming at 87C is flanked by a Chriz binding site on its proximal site only (Fig. 7b).

Chriz is essentially required for development

The ubiquitous overexpression of Chriz under the control of act-Gal4 and T80-Gal4 driver lines is early larval lethal. Da-Gal4 driven expression is semilethal and results in female sterility. Using different driver lines with a more restricted GAL4 expression pattern, organ- and tissue-

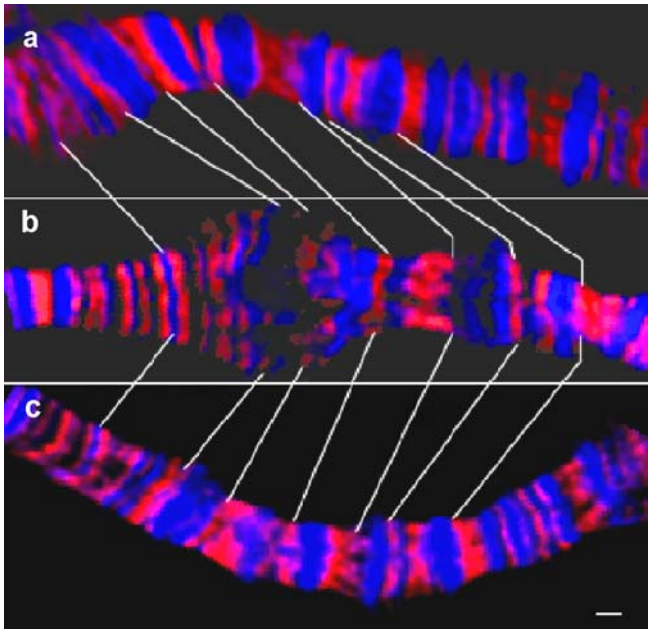

Fig. 7 Chriz chromosomal binding is largely unchanged by puff formation. Optical sections from the region 86–87 on the proximal chromosome 3R is shown in control (**a**, **c**) and experimental chromosomes (**b**) that were heat-shocked for 30 min at 37°C before fixation. Proximal towards *left*; Chriz antibody staining *red*, DNA staining *blue*. For clarity homologous loci are connected by *thin white lines* in the three micrographs. Note that Chriz remains localized at the distal side of the puff formed at 87A with some staining at the proximal side and on the proximal side of the puff forming at 87C; *bar* 0.8 μm

specific defects were observed indicating that a defined dosage of Chriz is essential for normal development (data not shown).

We obtained three independent stocks with P transposons integrated into the *Chriz* region (Fig. 1b; The FlyBase Consortium 2003; Bellen et al. 2004). In *KG6256* stock the *P{SUPor-P}* transposon was reported to be inserted 38 bp upstream of the first *Chriz* transcription start site. Flies homozygous for the *KG6256*-bearing chromosome normally die at the larval stage, but when cultivated at 16°C, rare adult escapers can be observed. In *KG3258*, the *P{SUPor-P}* transposon inserted into the *Chriz* first intron, 30 bp upstream of the second major transcription start site (Bellen et al. 2004). This insertion is homozygous embryonic lethal with rare first instar larvae escapers. Intriguingly, the *P{lacW}* insertion *sh044* (Oh et al. 2003) that occurred in exactly the same position as in *KG3258* is homozygous viable, and displays a female sterile phenotype. This might be attributed to the smaller size of the *P{lacW}* transposon, and the fact that it lacks the Su(Hw) binding sites present in *P{SUPor-P}*, which might interfere with proper promoter activity.

To prove that the phenotype observed was a result of the insertions of the transposons into the *Chriz* gene, we performed standard *P*-element excision crosses. In all three cases, we obtained numerous independent phenotypic revertant lines demonstrating that the lethality or sterility was induced by the corresponding *P* element insertions. Imprecise *P*-element excision events were registered as well, and in the same experiment we isolated 14 independent mutants that failed to complement each other and the original insertion strains. Furthermore, by complementation crosses we found that *Chriz* was uncovered by the deficiences *Df(3L)79E-F* and *Df(3L)Delta1AK* (79E5/F1–79F2/F6), but not by a more distal deficiency *Df(3L)HD1* (79D3/E1–79F3/6). This places the *Chriz* gene into the chromosomal region 79F3-6 in contrast to the data in the FlyBase that locate *Chriz* at 80B2.

According to the results of the interallelic and deficiency complementation, of 14 new *Chriz* alleles obtained by imprecise excision 11 are amorphic alleles and three are hypomorphs of various strength (Table 1). The breakpoints of the genomic aberrations in the most severe *Chriz* alleles were determined by Southern blotting and by sequencing the *Chriz* genomic region of the corresponding mutants (Fig. 1; Table 1). To exclude lethal hits unrelated to *Chriz* in the mutant stocks, complementation with a transgenic strain containing the 7.1-kb *Sca*I–*Eco*RI genomic fragment (Fig. 1) was carried out. The transgene contains *Chriz* and parts of the flanking genes and rescues most of the *Chriz* alleles. How-

Table 1 Classification and molecular characteristics of *Chriz* alleles

Allele designation	Stage of lethality / phenotype	Molecular data	Rescue by genomic clone	Allelic class
$Chriz^{KG3258}$	Embryonic-first instar larvae	Insertion of *P{SUPor-P}* transposon in the first intron	Yes	Amorph
$Chriz^{\Delta KG3}$		Incomplete excision of *P{SUPor-P}*		
$Chriz^{\Delta KG9}$		Deletion		
$Chriz^{\Delta KG12}$		2,737 bp of genomic sequence deleted with 14 bp of 5′ P-element end remaining		
$Chriz^{\Delta KG53}$		Incomplete *P{SUPor-P}* excision		
$Chriz^{\Delta KG65}$		1,135 bp of genomic sequence deleted with 35 bp of 5′ P-element end remaining		
$Chriz^{\Delta KG4}$	Adult escapers	Incomplete excision of *P{SUPor-P}*	Yes	Hypomorph
$Chriz^{\Delta KG6}$	Pupa			
$Chriz^{\Delta KG26}$	Imago escapers			
$Chriz^{sh044}$	Viable, female sterile	Insertion of *P{lacW}* in the first intron		
$Chriz^{KG6256}$	Lethal, rare imago escapers at +16C	Insertion of *P{SUPor-P}* in upstream of *Chriz*		
$Chriz^{\Delta KG10,\ 20,\ 30,\ 39}$	Embryonic-first instar larvae	Deletion of *Chriz* genomic material	No	Amorph, but accompanied by second site mutation

ever, the alleles $Chriz^{\Delta KG10}$, $Chriz^{\Delta KG20}$, $Chriz^{\Delta KG30}$, and $Chriz^{\Delta KG39}$ failed to be complemented by an ectopic *Chriz* copy. In fact, both $Chriz^{\Delta KG10}$ and $Chriz^{\Delta KG20}$ deletions not only removed the first transcription start site and the first exon of *Chriz*, they also affected the 5′-UTR of the neighboring *Ssl1* gene (Fig. 1; Table 1). Since our data demonstrate that $Chriz^{\Delta KG10}$, $Chriz^{\Delta KG20}$, $Chriz^{\Delta KG30}$ and $Chriz^{\Delta KG39}$ affect genes in addition to *Chriz*, these lines were not considered any further.

As indicated in Fig. 1, the $Chriz^{\Delta KG12}$ and $Chriz^{\Delta KG65}$ amorphic alleles leave the first transcription start site for *Chriz* intact, but completely remove the sequences comprising the second *Chriz* transcription start, along with the translation starting site up to the last 237 aa $\left(Chriz^{\Delta KG12}\right)$ or 630 aa, respectively $\left(Chriz^{\Delta KG65}\right)$. In neither case were sequences corresponding to the chromodomain retained. Therefore, we consider these alleles as null alleles.

Z4 and Chriz are largely independent of each other for chromosomal binding

The coimmunoprecipitation of Chriz with Z4 and the precise colocalization in diploid nuclei and polytene chromosomes suggest that both proteins bind to each other or that they occur in a common complex together with other proteins. However, the direct interaction between the two proteins when tested in the yeast two-hybrid system and by GST pulldown was rather weak (data not shown). To test whether the chromosomal binding of Z4 was dependent on Chriz, we used Chriz RNAi-induced knockdown driven by the G14.2-Gal4 driver line, which is specifically expressed in salivary glands (Fig. 8a, b). As shown in Fig. 8b, Chriz staining gives a strongly reduced signal on polytene chromosomes of these animals compared to its normal staining as seen in Fig 8c. However, although reduced, Chriz protein is still present in interbands. In contrast, the Z4 staining in interbands of such animals is similar to that in wild-type (Fig. 8a). We conclude that the chromosomal binding of Z4 is not exclusively dependent on Chriz. Conversely, animals heterozygous for the hypomorphic allele *Z4-7.1* and the null-allele *Z4-1.3* (Eggert et al. 2004) show a strongly reduced staining with Z4 antibodies (Fig. 8c) compared to the normal staining (Fig. 8a), but staining with anti-Chriz antisera is similar to that in wild-type (Fig. 8c; note that the images for Z4 in Fig. 8a, d and for Chriz in Fig. 8b, c were taken and reproduced under exactly the same conditions). This demonstrates that chromosomal binding of Chriz does not depend on Z4 either. In conclusion, our data suggest that both proteins colocalize by indirect interaction possibly in a chromatin complex.

Reducing the amount of Chriz protein does not induce a chromosomal phenotype

Z4 mutant alleles produce a chromosomal phenotype of a progressive loss of polytene chromosome structure at late third instar larval/early pupal stage (Eggert et al. 2004). Animals homozygous for amorphic *Chriz* alleles did not survive past first instar larval stage and could not be tested for a chromosomal phenotype. When Chriz was knocked down by induced RNAi in salivary glands, a chromosomal phenotype was not observed even at 29°C. However, although in such animals Chriz protein is strongly reduced it is not completely absent (Fig. 8b). We cannot exclude that the remaining Chriz protein is sufficient to support the structural integrity of polytene chromosomes. Unfortunately, the homozygotes for the available hypomorphic Chriz alleles expressed even more Chriz protein than the RNAi line and consequently also did not exhibit a chromosomal phenotype (not shown).

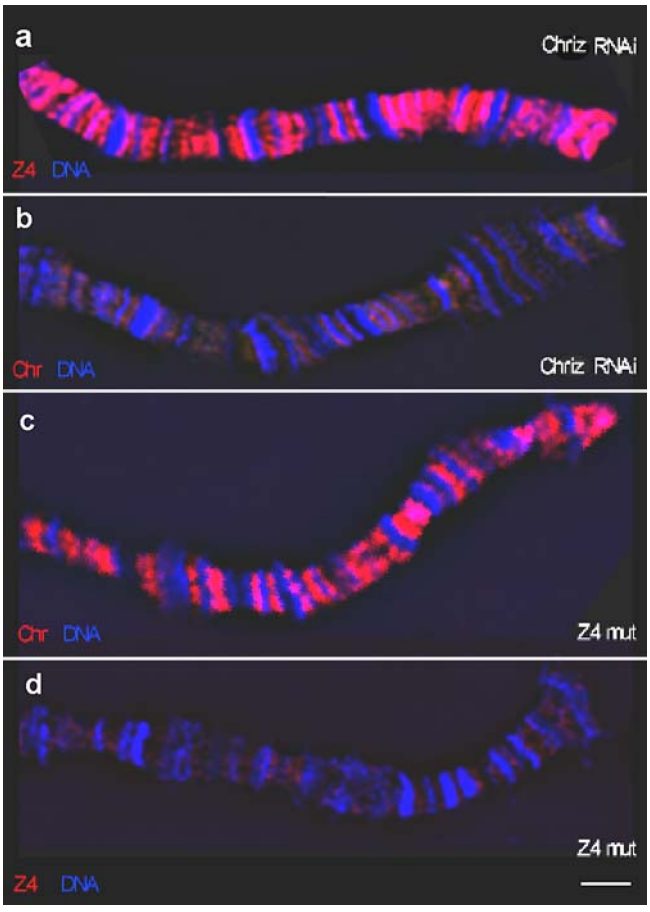

Fig. 8 Chriz and Z4 do not depend on each other for chromosomal binding. **a**, **b** Optical sections of chromosomes following knock down of Chriz by RNAi, DNA staining in *blue*; Z4 staining (*red*) shown in **a** as in wild-type, but Chriz staining (*red*) shown in **b** is strongly reduced; **c**, **d** optical sections of chromosomes from *Z4-1.3*/*Z4-7.1* larvae (*Z4* hypomorph), DNA staining in *blue*; Chriz staining (*red*) shown in **c** is as in wild-type, but Z4 staining (*red*) shown in **d** is strongly reduced; exposure is the same in all images shown and intensity values were set to the same scale. Note that the chromosomal phenotype of Z4 mutations is not seen in **c** and **d** since we used younger larvae that still have some Z4 protein; *bar* 2.5 μm

Discussion

We identified the chromodomain protein Chriz by co-immunoprecipitation in a protein complex with the zinc finger protein Z4. Both proteins colocalize in the nuclei of all *Drosophila* tissues tested so far and precisely colocalize on polytene interphase chromosomes. Although both proteins are readily coimmunoprecipitated, the observed direct interaction between the two proteins is surprisingly weak in vitro (M. Gan, unpublished data) and both proteins bind to polytene chromosomes largely independent of each other. Thus, we cannot exclude that the interaction between both proteins is indirect and coimmunoprecipitation is mediated by one of the other proteins coimmunoprecipitated with the Z4/Chriz complex. Mass spectrometry allowed the identification of one additional presumptive complex subunit, and it was characterized by immunostaining as an interband-specific protein (A. Gortchakov, unpublished data). Interestingly, the *Drosophila* homolog of the boundary element binding factor dCTCF (R. Renkawitz, Giessen, personal communication) found in a subset of interbands is coprecipitated with Chriz and Z4. In addition, BEAF32 (Zhao et al. 1995) and Jil-1 (Jin et al. 1999, 2000) colocalize with Chriz and Z4 in many interbands in an overlapping, although not identical, pattern (H. Saumweber, unpublished data). Work is in progress to shed more light on these interactions and their functional relevance.

More recently, the same protein was independently identified by Rath et al. (2004), who called this protein Chromator. Chromator was identified because of the interaction of its carboxyterminal domain with Skeletor, an essential component of the mitotic spindle. The authors demonstrated strong binding of this protein to the mitotic spindle and to centrosomes, which was corroborated by our results. They also demonstrated by RNA interference in S2 cells that this protein is involved in spindle organization during mitosis. However, the specific chromosomal binding in diploid cells and on polytene chromosomes and the presence of a chromodomain suggest a function in interphase chromatin as well.

Chriz is essential as demonstrated by the isolation of new loss of function alleles and we observed that increasing the dosage of this protein is not tolerated either. Unlike Z4, reducing the dosage of Chriz did not result in a chromosomal phenotype. Neither depletion of the Chriz protein by hypomorphic mutations nor by RNA interference resulted in abnormal chromosome morphology. However, in both cases detectable Chriz protein remained that was bound with the same specificity as in wild-type. Complete loss of Chriz cannot be tested since amorphic alleles are embryo/first larval lethal.

It is still not known what mediates the specific binding of Z4 and Chriz to interbands. The zinc finger protein Z4 showed a general affinity for DNA binding and the specificity of pairs of zinc fingers from that protein is currently being tested. Yet, as suggested by our results, Z4 alone does not determine the specific chromosomal targeting of Chriz. On the other hand, DNA binding of Chriz has not been studied; however, with the exception of dMi-2 (Bouazoune et al. 2002), chromodomain-containing proteins were not shown to bind DNA. Rather, they bind to modified nucleosomes or chromosomal RNA (Akhtar et al. 2000). Experiments are in progress to uncover the domain of Chriz required for chromosomal binding. As first demonstrated for HP1 and PC, chromodomains mediate the binding to methylated histones (Nielsen et al. 2002; Fischle et al. 2003). HP1 binds di- and trimethylated H3K9 and PC binds di- and trimethylated H3K27 and/or H3K9 (Fischle et al. 2003; Czermin et al. 2002; Ringrose et al. 2004). However, due to the lack of two essential aromatic residues, the Chriz chromodomain may be not involved in binding to di- and trimethylated H3K9 and H3K27; in fact, no binding was observed in the chromocenter core and pericentric chromatin that is rich in these histone modifications (Ebert et al. 2004). Similarly, binding to trimethylated H4K20 (Schotta et al. 2004) is unlikely due to the lack of Chriz staining of pericentric heterochromatin. At present, however, binding of the Chriz chromodomain to other methyl marks on histones cannot be ruled out. In particular, it would be interesting to see if it binds to activating methylation modifications such as methylated H3K4 (Santos-Rosa et al. 2002; Byrd and Shearn 2003). Binding to chromosomal RNA may be considered as an alternative. The MOF and MSL3 components of the *Drosophila* dosage compensation complex contain a chromodomain that binds to RNA in vitro and is important to target these proteins to many interbands on the X chromosome by formation of complexes with the noncoding roX1 and roX2 RNAs (Akhtar 2003). Having chromodomains with different specificity/affinity to RNAs locally present on chromosomes would provide an attractive alternative targeting mechanism.

Acknowledgements The authors thank I. Passow and R. Gienapp for excellent technical assistance. We acknowledge the help of K. Matthews from Bloomington Stock Center for provision of fly stocks and A. Carpenter for her kind gift of the transposase donor stock. I.F. Z. and A.A.G. were supported by a short-term DAAD Scholarship, by Programs for Molecular and Cellular Biology 10.1 and N70/2004, Program for Scientific Schools 918.2003, and by a grant Frontiers in Genetics 2-04. H.E. and H.S. were supported by a grant from DFG Sa338/9-1 Schwerpunkt Epigenetics.

References

Akhtar A (2003) Dosage compensation: an intertwined world of RNA and chromatin remodelling. Curr Opin Genet Dev 13: 161–169

Akhtar A, Zink D, Becker PB (2000) Chromodomains are protein–RNA interaction modules. Nature 407:405–409

Altschul M, Simpson KW, Dykes NL, Mauldin EA, Reubi JC, Cummings JF (1997) Gapped BLAST and PSI-BLAST: a new generation of protein database search programs. Nucleic Acids Res 25:3389–3402

Arbeitman MN, Furlong EE, Imam F, Johnson E, Null BH, Baker BS, Krasnow MA, Scott MP, Davis RW, White KP (2002) Gene expression during the life cycle of *Drosophila melanogaster*. Science 297:2270–2275

Armstrong JA, Papoulas O, Daubresse G, Sperling AS, Lis JT, Scott MP, Tamkun JW (2002) The Drosophila BRM complex facilitates global transcription by RNA polymerase II. EMBO J 21: 5245–5254

Beermann W (1972) Chromomeres and genes. In: Beermann W, Reiner J, Ursprium H (eds) Results and problems in cell differentiation, vol 4. Springer, Berlin Heidelberg New York, pp 1–33

Bellen HJ, Levis RW, Liao G, He Y, Carlson JW, Tsang G, Evans-Holm M, Hiesinger PR, Schulze KL, Rubin GM, Hoskins RA, Spradling AC (2004) The BDGP gene disruption project: single transposon insertions associated with 40% of Drosophila genes. Genetics 167:761–781

Benyajati C, Worcel A (1976) Isolation, characterization, and structure of the folded interphase genome of *Drosophila melanogaster*. Cell 9:393–407

Bier E, Vaessin H, Shepherd S, Lee K, McCall K, Barbel S, Ackerman L, Carretto R, Uemura T, Grell E (1989) Searching for pattern and mutation in the Drosophila genome with a P-lacZ vector. Genes Dev 3:1273–1287

Bouazoune K, Mitterweger A, Langst G, Imhof A, Akhtar A, Becker PB, Brehm A (2002) The dMi-2 chromodomains are DNA binding modules important for ATP-dependent nucleosome mobilization. EMBO J 21:2430–2440

Brand AH, Perrimon N (1993) Target gene expression as a means of altering cell fates and generating dominant phenotypes. Development 118:401–415

Byrd NK, Shearn A (2003) ASH1, a Drosophila trithorax group protein, is required for methylation of lysine 4 residues on histone H3. Proc Natl Acad Sci U S A 100:11535–11540

Callan HG (1987) Lampbrush chromosomes as seen in historical perspective. In: Hennig W (ed) Results and problems in cell differentiation, vol 14. Structure and function of eukaryotic chromosomes. Springer, Berlin Heidelberg New York, pp 5–26

Cherbas L, Hu X, Zhimulev I, Belyaeva E, Cherbas P (2002) EcR isoforms in Drosophila: testing tissue-specific requirements by targeted blockade and rescue. Development 130:271–284

Clegg NJ, Frost DM, Larkin MK, Subrahmanyan L, Bryant Z, Ruohola-Baker H (1997) Maelstrom is required for an early step in the establishment of Drosophila oocyte polarity: posterior localization of grk mRNA. Development 124:4661–4671

Corpet F (1988) Multiple sequence alignment with hierarchical clustering. Nucleic Acids Res 16(22):10881–10890

Cuvier O, Hart CM, Laemmli UK (1998) Identification of a class of chromatin boundary elements. Mol Cell Biol 18:7478–7486

Czermin B, Melfi R, McCabe D, Steitz V, Imhof A, Pirrotta V (2002) Drosophila enhancer of Zeste/ESC complexes have a histone H3 methyltransferase activity that marks chromosomal Polycomb sites. Cell 111:185–196

Ebert A, Schotta G, Lein S, Kubicek S, Krauss V, Jenuwein T, Reuter G (2004) Su(var) genes regulate the balance between euchromatin and heterochromatin in Drosophila. Genes Dev 18:2973–2983

Eggert H, Gortchakov A, Saumweber H (2004) Identification of the *Drosophila* interband-specific protein Z4 as a DNA-binding zinc-finger protein determining chromosomal structure. J Cell Sci 117:4253–4264

Fischle W, Wang Y, Jacobs SA, Kim Y, Allis CD, Khorasanizadeh S (2003) Molecular basis for the discrimination of repressive methyl-lysine marks in histone H3 by Polycomb and HP1 chromodomains. Genes Dev 17:1870–1881

Frasch M, Glover DM, Saumweber H (1986) Nuclear antigens follow different pathways into daughter nuclei during mitosis in early Drosophila embryos. J Cell Sci 82:155–172

Gerber M, Ma J, Dean K, Eissenberg JC, Shilatifard A (2001) Drosophila ELL is associated with actively elongating RNA polymerasse II on transcriptionally active sites in vivo. EMBO J 20:6104–6114

Hart CM, Zhao K, Laemmli UK (1997) The scs′ boundary element: characterization of boundary element-associated factors. Mol Cell Biol 17(2):999–1009

Hoskins RA, Nelson CR, Berman BP, Laverty TR, George RA, Ciesiolka L, Naeemuddin M, Arenson AD, Durbin J, David RG, Tabor PE, Bailey MR, DeShazo DR, Catanese J, Mammoser A, Osoegawa K, de Jong PJ, Celniker SE, Gibbs RA, Rubin GM, Scherer SE (2000) A BAC-based physical map of the major autosomes of *Drosophila melanogaster*. Science 287:2271–2274

Hovemann BT, Reim I, Werner S, Katz S, Saumweber H (2000) The protein Hrb57A of *Drosophila melanogaster* closely related to hnRNP K from vertebrates is present at sites active in transcription and coprecipitates with four RNA-binding proteins. Gene 245:127–137

Igo-Kemenes T, Zachau HG (1978) Domains in chromatin structure. Cold Spring Harb Symp Quant Biol 42:109–118

Ito K, Sass H, Urban J, Hofbauer A, Schneuwly S (1997) GAL4-responsive UAS-tau as a tool for studying the anatomy and development of the Drosophila central nervous system. Cell Tissue Res 290:1–10

Jin Y, Wang Y, Walker DL, Dong H, Conley C, Johansen J, Johansen KM (1999) JIL-1: a novel chromosomal tandem kinase implicated in transcriptional regulation in Drosophila. Mol Cell 4:129–135

Jin Y, Wang Y, Johansen J, Johansen KM (2000) JIL-1, a chromosomal kinase implicated in the regulation of chromatin structure, associates with the male specific lethal (MSL) dosage compensation complex. J Cell Biol 149:1005–1010

Kellum R, Schedl P (1991) A position-effect assay for boundaries of higher order chromosomal domains. Cell 64:941–950

Kellum R, Schedl P (1992) A group of scs elements function as domain boundaries in an enhancer-blocking assay. Mol Cell Biol 12:2424–2431

Lindsley DL, Zimm GG (1992) The genome of *Drosophila melanogaster*. Academic, San Diego

Mohrmann L, Langenberg K, Krijgsveld J, Kal AJ, Heck AJ, Verrijzer CP (2004) Differential targeting of two distinct SWI/SNF-related Drosophila chromatin-remodeling complexes. Mol Cell Biol 24:3077–3088

Nielsen PR, Nietlispach D, Mott HR, Callaghan J, Bannister A, Kouzarides T, Murzin AG, Murzina NV, Laue ED (2002) Structure of the HP1 chromodomain bound to histone H3 methylated at lysine 9. Nature 416:403–407

O'Connell PO, Rosbash M (1984) Sequence, structure, and codon preference of the Drosophila ribosomal protein 49 gene. Nucleic Acids Res 12:5495–5513

Oh SW, Kingsley T, Shin HH, Zheng Z, Chen HW, Chen X, Wang H, Ruan P, Moody M, Hou SX (2003) A P-element insertion screen identified mutations in 455 novel essential genes in Drosophila. Genetics 163:195–201

Paddy MR, Saumweber H, Agard DA, Sedat JW (1996) Time-resolved, in vivo studies of mitotic spindle formation and nuclear lamina breakdown in Drosophila early embryos. J Cell Sci 109:591–607

Paro R, Hogness DS (1991) The Polycomb protein shares a homologous domain with a heterochromatin-associated protein of Drosophila. Proc Natl Acad Sci U S A 88:263–267

Paulson JR, Laemmli UK (1977) The structure of histone-depleted metaphase chromosomes. Cell 12:817–828

Plagens U, Greenleaf AL, Bautz EKF (1976) Distribution of RNA Polymerase on Drosophila polytene chromosomes studied by indirect immunofluorescence. Chromosoma 59:157–165

Rath U, Wang D, Ding Y, Xu YZ, Qi H, Blacketer MJ, Girton J, Johansen J, Johansen K (2004) Chromator, a novel and essential chromodomain protein interacts directly with the putative spindle matrix protein Skeletor. J Cell Biochem 93(5):1033–1047

Reim I, Mattow J, Saumweber H (1999) The RRM protein NonA from Drosophila forms a complex with the RRM proteins Hrb87F and S5 and the Zn finger protein PEP on hnRNA. Exp Cell Res 253:573–586

Ringrose L, Ehret H, Paro R (2004) Distinct contributions of histone H3 Lysine 9 and 27 methylation to locus-specific stability of polycomb complexes. Mol Cell 16:641–653

Roseman RR, Johnson EA, Rodesch CK, Bjerke M, Nagoshi RN, Geyer PK (1995) A P-element containing suppressor of hairy-wing binding regions has novel properties for mutagenesis in *Drosophila melanogaster*. Genetics 141:1061–1074

Rubin GM, Yandell MD, Wortman JR, Gabor Miklos GL, Nelson CR, Hariharan IK, Fortini ME, Li PW, Apweiler R, Fleischmann W, Cherry JM, Henikoff S, Skupski MP, Misra S, Ashburner M, Birney E, Boguski MS, Brody T, Brokstein P, Celniker SE, Chervitz SA, Coates D, Cravchik A, Gabrielian A, Galle RF, Gelbart WM, George RA, Goldstein LS, Gong F, Guan P, Harris NL, Hay BA, Hoskins RA, Li J, Li Z, Hynes RO, Jones SJ, Kuehl PM, Lemaitre B, Littleton JT, Morrison DK, Mungall C, O'Farrell PH, Pickeral OK, Shue C, Vosshall LB, Zhang J, Zhao Q, Zheng XH, Lewis S (2000) Comparative genomics of the eukaryotes. Science 287:2204–2215

Rykowski MC, Parmelee SJ, Agard DA, Sedat JW (1988) Precise determination of the molecular limits of a polytene chromosome band: regulatory sequences for the Notch gene are in the interband. Cell 54:461–472

Sambrook J, Russell DW (2001) Molecular cloning: a laboratory manual. Cold Spring Harbor Laboratory Press, New York

Santos-Rosa H, Schneider R, Bannister AJ, Sherriff J, Bernstein BE, Emre NCT, Schreiber SL, Mellor JU, Kouzarides T (2002) Active genes are trimethylated at K4 of histone H3. Nature 419:407–411

Sass H (1982) RNA polymerase B in polytene chromosomes: immunofluorescent and autoradiographic analysis during stimulated and repressed RNA synthesis. Cell 28:269–278

Sass H, Bautz EKF (1982) Interbands of polytene chromosomes: binding sites and start points for RNA polymerase. Chromosoma 86:77–93

Schotta G, Lachner M, Sarma K, Ebert A, Sengupta R, Reuter G, Reinberg D, Jenuwein T (2004) A silencing pathway to induce H3-K9 and H3-K20 trimethylation at constitutive heterochromatin. Genes Dev 18:1251–1262

Semeshin VF, Zhimulev IF, Belyaeva ES (1979) Electron microscope autoradiographic study on transcriptional activity of *Drosophila melanogaster* polytene chromosomes. Chromosoma 73:163–177

Smoller D, Friedel C, Schmid A, Bettler D, Lam L, Yedvobnick B (1990) The Drosophila neurogenic locus mastermind encodes a protein unusually rich in aminoacid homopolymers. Genes Dev 4:1688–1700

The FlyBase Consortium (2003) The FlyBase database of the Drosophila genome projects and community literature. Nucleic Acids Res 31:172–175. (http://www.flybase.net/)

Udvardy A, Maine E, Schedl P (1985) The 87A7 chromomere. Identification of novel chromatin structures flanking the heat shock locus that may define the boundaries of higher order domains. J Mol Biol 20:341–358

Vazquez J, Schedl P (2000) Deletion of an insulator element by the mutation facet-strawberry in *Drosophila melanogaster*. Genetics 155:1297–1311

Weeks JR, Hardin SE, Shen J, Lee JM, Greenleaf AL (1993) Locus-specific variation in phosphorylation state of RNA polymerase II in vivo: correlations with gene activity and transcript processing. Genes Dev 7:2329–2344

Wilder EL, Perrimon N (1995) Dual functions of wingless in the Drosophila leg imaginal disc. Development 121:477–488

Wodarz A, Hinz U, Engelbert M, Knust E (1995) Expression of crumbs confers apical character on plasma membrane domains of ectodermal epithelia of Drosophila. Cell 82:67–76

Zhao K, Hart CM, Laemmli UK (1995) Visualization of chromosomal domains with boundary element-associated factor BEAF-32. Cell 81:879–889

Zhimulev IF (1996) Morphology and structure of polytene chromosomes. Adv Genet 34:1–497

Zhimulev IF, Belyaeva ES (1975) ^{3}H-uridine labeling patterns in the *Drososphila melanogaster* salivary gland chromosomes X, 2R and 3L. Chromosoma 49:219–231